Molecular Microbiology (2008) 67(5), 1125–1142 ■
doi:10.1111/j.1365-2958.2008.06112.x
First published online 23 January 2008

Mitochondrial fatty acid synthesis is required for normal mitochondrial morphology and function in *Trypanosoma brucei*

Jennifer L. Guler,[1] Eva Kriegova,[2] Terry K. Smith,[3†] Julius Lukeš[2] and Paul T. Englund[1*]
[1]*Department of Biological Chemistry, Johns Hopkins University School of Medicine, Baltimore, MD, USA.*
[2]*Institute of Parasitology, Czech Academy of Sciences, and Faculty of Science, University of South Bohemia, České Budějovice, Czech Republic.*
[3]*Division of Biological Chemistry and Drug Discovery, Wellcome Trust Biocentre, College of Life Sciences, University of Dundee, Dundee, Scotland.*

Summary

Trypanosoma brucei **use microsomal elongases for *de novo* synthesis of most of its fatty acids. In addition, this parasite utilizes an essential mitochondrial type II synthase for production of octanoate (a lipoic acid precursor) as well as longer fatty acids such as palmitate. Evidence from other organisms suggests that mitochondrially synthesized fatty acids are required for efficient respiration but the exact relationship remains unclear. In procyclic form trypanosomes, we also found that RNAi depletion of the mitochondrial acyl carrier protein, an important component of the fatty acid synthesis machinery, significantly reduces cytochrome-mediated respiration. This reduction was explained by RNAi-mediated inhibition of respiratory complexes II, III and IV, but not complex I. Other effects of RNAi, such as changes in mitochondrial morphology and alterations in membrane potential, raised the possibility of a change in mitochondrial membrane composition. Using mass spectrometry, we observed a decrease in total and mitochondrial phosphatidylinositol and mitochondrial phosphatidylethanolamine. Thus, we conclude that the mitochondrial synthase produces fatty acids needed for maintaining local phospholipid levels that are required for activity of respiratory complexes and preservation of mitochondrial morphology and function.**

Introduction

Trypanosoma brucei is the protozoan parasite that causes nagana in cattle and African sleeping sickness in humans. Two of its life cycle stages are easily cultured in the laboratory; the procyclic form (PCF) normally resides in the midgut of the tsetse vector and the bloodstream form (BSF), which causes disease, multiplies within the mammalian bloodstream. Over the years a major objective of trypanosome research has been to identify novel drug targets. As a result, many investigators have focused on the atypical biology of this parasite, which differs markedly from that of its mammalian host. One unusual feature is the single tubular mitochondrion that extends throughout the cell and houses indispensable metabolic pathways. PCF trypanosomes, the focus of these studies, are mostly fuelled by amino acids catabolized in this organelle (van Weelden *et al.*, 2003; van Weelden *et al.*, 2005). However, when glucose is available, it is catabolized in the glycosome, a peroxisome-like organelle which houses most of the glycolytic pathway (Opperdoes and Borst, 1977). Pyruvate, the end-product of glycolysis, is produced in the cytosol and further metabolized within the mitochondrion (Lamour *et al.*, 2005; Bringaud *et al.*, 2006).

An atypical feature of the PCF mitochondrion is its branched respiratory chain. Ubiquinone can carry electrons from succinate dehydrogenase (complex II) [and potentially from NADH:ubiquinone oxidoreductase (complex I) and alternative NADH dehydrogenases (Fang and Beattie, 2002, 2003a)] either to the cytochrome-mediated respiratory chain [involving cytochrome *c* reductase (complex III), cytochrome *c* and cytochrome *c* oxidase (complex IV)] or to the trypanosome alternative oxidase (TAO) (Hill and Cross, 1973; Njogu *et al.*, 1980). As KCN inhibits the former and salicylhydroxamic acid (SHAM) the latter, both inhibitors are required to block respiration completely (Njogu *et al.*, 1980; van Weelden *et al.*, 2003) (Fig. 3A).

Although a multisubunit complex I has recently been characterized in *Phytomonas serpens*, a plant parasite

Accepted 2 January, 2008. *For correspondence. E-mail penglund@jhmi.edu; Tel. (+1) 410 955 3458; Fax (+1) 410 955 7810. †Present address: Centre for Biomolecular Sciences, The North Haugh, The University, St. Andrews. KY16 9ST, Scotland, UK.

related to trypanosomes, the presence of a typical complex I in *T. brucei* is controversial (for discussion see Čermáková *et al*., 2007). If present, it may be smaller and highly diverged from its counterpart in higher eukaryotes. Alternatively, *T. brucei* may have bypassed the need for complex I all together. Instead, it may use an NADH-fumarate reductase to oxidize mitochondrial NADH, thereby producing succinate as a substrate for complex II (Turrens, 1989).

Another remarkable feature of trypanosome metabolism is their mechanism for *de novo* synthesis of fatty acids. While most eukaryotic organisms utilize a multi-domain type I cytoplasmic fatty acid synthase (Smith, 1994), trypanosomes instead use an unconventional family of elongases (ELO) to assemble saturated fatty acids up to stearate (C18) (Lee *et al*., 2006). However, like other eukaryotes (Mikolajczyk and Brody, 1990; Shintani and Ohlrogge, 1994; Gueguen *et al*., 2000), the trypanosome mitochondrion also houses a prokaryotic-like type II fatty acid synthase. In this synthase, all catalytic activities, as well as acyl carrier protein (ACP), reside on separate polypeptides. Mitochondrial synthases make the octanoate (C8) precursor of lipoic acid (Brody *et al*., 1997; Gueguen *et al*., 2000; Stephens *et al*., 2007), a cofactor for mitochondrial α-ketoacid dehydrogenase complexes. Longer fatty acids, such as myristate (C14) in fungi (Mikolajczyk and Brody, 1990), palmitate (C16) in trypanosomes (Stephens *et al*., 2007) and stearate (C18) in plants (Shintani and Ohlrogge, 1994; Gueguen *et al*., 2000), are also synthesized intramitochondrially. Mitochondrial fatty acid synthesis appears to be required for normal respiratory function, which in some cases, is explained by the fact that ACP is an essential component of complex I (Runswick *et al*., 1991; Sackmann *et al*., 1991; Schneider *et al*., 1995; Cronan *et al*., 2005). However, ACP depletion in *Saccharomyces cerevisiae,* an organism naturally devoid of complex I, also decreases respiration (Schneider *et al*., 1995; Hiltunen *et al*., 2005), and this finding suggests a relationship between products of the mitochondrial fatty acid synthase and respiration.

In PCF trypanosomes, RNAi knock-down of ACP resulted in inhibition of cytochrome-mediated respiration, causing the cells to rely more on the SHAM-sensitive alternative oxidase. Like *S. cerevisiae*, we found that the respiratory inhibition was independent of an effect on complex I. In addition, ACP depletion in trypanosomes caused phenotypic changes in mitochondrial membrane potential and ultrastructure that we attribute to the alteration in mitochondrial phospholipid composition. Thus, the mitochondrial fatty acid synthase plays a key role in mitochondrial function by supplying the fatty acids needed for maintenance of local phospholipids, ensuring organellar integrity and proper functioning of the respiratory machinery.

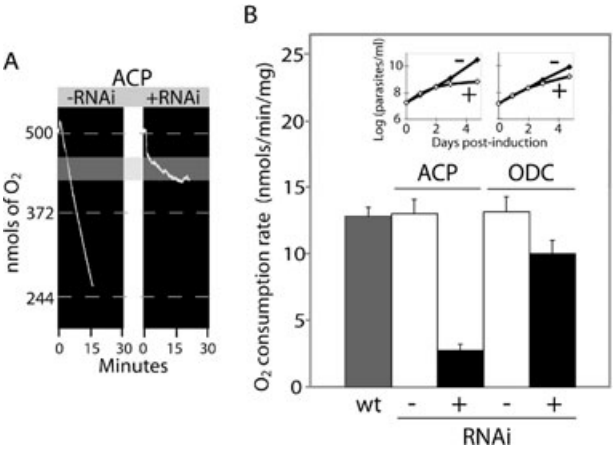

Fig. 1. Effect of ACP RNAi on respiration.
A. O_2 electrode traces from uninduced (–RNAi) and induced (3 days, +RNAi) ACP RNAi trypanosomes. The O_2 consumption rate from a representative experiment was calculated from the slope of the line in the light grey region of the trace [–RNAi: 9.7 nmol min^{-1} (mg protein)$^{-1}$, +RNAi: 1.3 nmol min^{-1} (mg protein)$^{-1}$]. For the above calculations, we assumed the solubility of oxygen in water at 28°C is 250 μM.
B. Mean O_2 consumption rates (± standard error) from wild-type cells (untransfected strain 29–13, grey bar, $n = 11$), uninduced ACP RNAi cells (white bar, $n = 10$) and ACP RNAi cells induced for 2–4 days (black bar, $n = 15$). As a control, we included average rates from either ODC RNAi cells uninduced (white bar, $n = 5$) or induced for 3–4 days (black bar, $n = 10$). In agreement with published data (Wang *et al*., 2000; Stephens *et al*., 2007), growth curves show that RNAi of ACP (left inset) and ODC (right inset) caused a growth defect starting at day 3. Parasites per ml (*Y*-axis) was calculated by multiplying cell density and dilution factor. Tetracycline (1 μg ml^{-1}) was added at 0 h to induce RNAi.

Results

ACP RNAi inhibits respiration

In *S. cerevisiae*, mitochondrial fatty acid synthesis is essential for respiratory competence (Hiltunen *et al*., 2005). To determine if the same is true in PCF *T. brucei*, we compared O_2 consumption rates [(nmol O_2) min^{-1} (mg protein)$^{-1}$] in cells having normal levels of ACP with those having ACP levels knocked-down by RNAi. A representative O_2 electrode trace revealed a clear defect in O_2 consumption following 3 days of ACP RNAi (Fig. 1A). Averaging results from several experiments, we found that uninduced RNAi cells respired at a rate comparable to that of wild-type cells (13.1 ± 1.1 and 12.8 ± 0.7 nmol min^{-1} mg^{-1} respectively). In contrast, respiration of RNAi cells (induced for 2–4 days) was reduced by ~80% (2.8 ± 0.5 nmol min^{-1} mg^{-1}) (Fig. 1B). To be certain that the effect on respiration was due to ACP level and not just to reduction in the growth rate, we also measured O_2 consumption following knock-down of another essential enzyme, ornithine decarboxylase (ODC) (Wang *et al*., 2000). Although the growth effect in both RNAi cell lines started 3 days after induction of RNAi (inset graphs in Fig. 1B), O_2 consump-

Table 1. Activity assays (mean ± standard deviation) of respiratory complexes following 3 or 5 days of ACP RNAi.

	Respiratory complex	Days +RNAi	–RNAi specific activity[a]	% of –RNAi
NADH dehydrogenase	I (Fe)[b]	0	182 ± 41 U mg^{-1}	100%
		3		79 ± 15
		5		72 ± 17
	I (Q_2)[b]	0	50 ± 14 U mg^{-1}	100%
		3		82 ± 4
		5		83 ± 6
Succinate dehydrogenase	II	0	38 ± 22 U mg^{-1}	100%
		3		34 ± 9
		5		26 ± 10
Cytochrome *c* reductase	III	0	192 ± 89 mU mg^{-1}	100%
		3		77 ± 11
		5		33 ± 7
Cytochrome *c* oxidase	IV	0	1.4 ± 0.5 mU mg^{-1}	100%
		3		74 ± 9
		5		56 ± 12
ATP synthase	V	0	353 ± 122 U mg^{-1}	100%
		3		84 ± 5
		5		93 ± 13

a. For NADH-dehydrogenase, a unit is defined as the amount of enzyme that oxidizes 1 nmol NADH per minute (González-Halphen and Maslov, 2004). For succinate-dehydrogenase, a unit is defined as the amount of enzyme that oxidizes 1 nmol of 2,6-dichlorphenolindolphenol per minute (Birch-Machin and Turnbull, 2001). For cytochrome *c*-reductase/oxidase, a milliunit is defined as the amount of enzyme that reduces or oxidizes 1 μmol of cytochrome *c* per minute (Horváth *et al*., 2000). For ATP-synthase the reverse reaction is measured and a unit is defined as the amount of enzyme that releases 1 nmol of inorganic phosphate per minute (Law *et al*., 1995).
b. Ferricyanide (Fe) or ubiquinone 2 (Q_2) were used as two different artificial electron acceptors to measure NADH dehydrogenase activity.
% of –RNAi was calculated using values from uninduced controls (–RNAi rate). Specific activity is units or milliunits/milligram of mitochondrial protein (U mg^{-1} or mU mg^{-1}).

tion (comparing uninduced and RNAi cells induced for 3–4 days) was only reduced by 24% after ODC RNAi (13.2 ± 1.3 and 10.1 ± 1.0 nmol min^{-1} mg^{-1} respectively) (Fig. 1B). Therefore, we conclude that trypanosomal mitochondrial ACP, as in other organisms, is required for efficient respiration.

As mitochondrial ACP is essential for the assembly and function of respiratory complex I in mammals and fungi (Runswick *et al*., 1991; Sackmann *et al*., 1991; Schneider *et al*., 1995; Cronan *et al*., 2005), we next investigated whether the RNAi-dependent respiratory defect was due to a specific effect on this complex. Spectrophotometric assays of NADH dehydrogenase activity revealed only a modest decrease (to 83% and 72% of wild-type levels, depending on the electron acceptor) after 5 days of RNAi (Table 1). It is possible that alternative NADH dehydrogenases (Fang and Beattie, 2002) could compensate for the loss of complex I activity in this assay. Therefore, we used a more specific assay for detection of the large, multisubunit complex I (Horváth *et al*., 2005) based on fractionation of mitochondrial lysates on a blue-native PAGE gel, followed by in-gel detection of complex I activity. Similar to spectrophotometric assays, we consistently observed a slight decrease in activity after 5 days (Fig. 2A, lane 5), when compared with uninduced cells (lane 3). However, when compared with wild-type activity (lane 2), there was a consistent increase in activity in uninduced cells (lane 3) and RNAi cells induced for 3 days (lane 4) or even 5 days (lane 5).

As ACP RNAi did not drastically reduce complex I activity, we next determined its effect on activity of the other

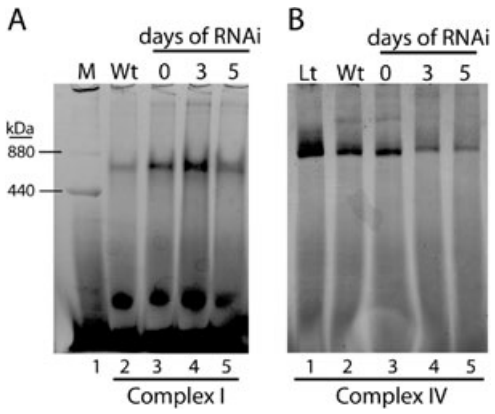

Fig. 2. Effect of ACP RNAi on the activity of respiratory complexes. Extracts of mitochondrial vesicles from trypanosomes (induced for ACP RNAi for 0, 3 or 5 days) were fractionated by blue native PAGE.
A. In-gel assay of complex I (NADH dehydrogenase) activity; M, molecular mass marker [880 kDa: ferritin dimer (equine spleen), 440 kDa: ferritin monomer)]. Wt, wild type control (untransfected strain 29–13).
B. In-gel assay of complex IV (cytochrome *c* oxidase) activity; Lt, *Leishmania tarentolae* control.

respiratory complexes. Spectrophotometric assays of complexes II and III after 5 days of RNAi showed a strong decrease in activity (to 26% and 33% of uninduced levels; Table 1). In addition, both in-gel and spectrophotometric assays showed that ACP RNAi caused complex IV activity to decrease by about half (Table 1 and Fig. 2B, compare lane 3 with lanes 4 and 5). There was no significant decrease in complex V activity (Table 1) but effects on complexes II, III and IV explain the reduction in respiration following ACP RNAi.

Effect of ACP RNAi and respiratory inhibitors on cell growth

To further assess the consequences of ACP depletion, we determined the effect of respiratory inhibitors on cell growth. Normally, PCF trypanosomes rely on both cytochrome-mediated and alternative respiratory pathways (Hill and Cross, 1973; Njogu *et al*., 1980; van Weelden *et al*., 2003) (see schematic diagram in Fig. 3A). This codependency is illustrated in the left panel of Fig. 3B; treating uninduced cells (–RNAi, none) with either 1 mM KCN (a complex IV inhibitor) or 1 mM SHAM (a TAO inhibitor) causes only partial growth inhibition (the doubling time of each increases by approximately twofold; note that all slopes were measured within the grey region of the growth curve), whereas treatment with both inhibitors completely stopped growth. As ACP is essential for growth of trypanosomes (Stephens *et al*., 2007), their doubling time is increased by approximately fourfold after RNAi induction (right panel, +RNAi, none). In these conditions, KCN treatment only partly inhibited cell growth (the doubling time was increased by less than twofold) but SHAM treatment inhibited growth completely. The increased sensitivity to SHAM [also observed by measuring its effect on O_2 consumption (J. Lukeš, unpubl.)], indicates that the RNAi cells have become more reliant on the alternative branch of the respiratory pathway. Consistent with this hypothesis, we found that cells undergoing ACP RNAi have increased levels of TAO, the terminal oxidase of the alternative branch. Using the standard chemiluminescent detection method, TAO protein was not visible in uninduced cells, but could only be seen after 4–5 days of RNAi (Fig. 3C, row 3). However, a more sensitive chemiluminescent method (Supersignal West Femto) revealed that TAO was dramatically upregulated between 3 and 4 days of RNAi (row 4). Levels of other mitochondrial proteins such as HSP-70 (row 1) and ATP synthase (row 2), however, changed little after ACP RNAi induction.

ACP RNAi alters mitochondrial membrane potential

Previous studies had shown that inactivation of trypanosome respiratory complexes, particularly III, IV and V, reduced mitochondrial staining by membrane potential-sensitive dyes (Horváth *et al*., 2005; Schnaufer *et al*., 2005; Brown *et al*., 2006). Because of the striking effects ACP depletion had on trypanosome respiration (Figs 1,2 and 3 and Table 1), we hypothesized that mitochondrial membrane potential would also be reduced in these cells. Therefore, we applied a method used previously to assess membrane potential in this organism (Timms *et al*., 2002; Brown *et al*., 2006); trypanosomes are stained with the membrane potential-dependant Mitotracker Red and observed by fluorescence microscopy. In wild-type cells, Mitotracker staining revealed the characteristic tubular pattern of a mitochondrion reflecting normal membrane potential (Fig. 4A, wt). Occasionally in these cells, there were bright spots where the Mitotracker dye had been concentrated (arrowhead, wt and day 0). In addition, we noticed a difference in the Mitotracker staining pattern between wild-type and uninduced RNAi cells: the mitochondrion changed from distinct tubules (wt) to thinner, net-like branches (day 0 and continuing to day 1, the asterisk '*'). This observation, along with the upregulation of complex I activity mentioned above, may be due to a slight leakiness in the expression of double-stranded RNA at day 0 and thus, indicate that the initial phenotype of ACP RNAi resembles the small, spindly networks of mitochondria found in yeast mitochondrial fatty acid synthesis knockouts (Torkko *et al*., 2001; Kastaniotis *et al*., 2004). The Mitotracker bright spots, however, became more prevalent at days 2 and 3 and then enlarged at day 4 of RNAi (arrow). Quantitative analysis showed that the average number of Mitotracker bright spots per cell progressively increased from ~1 in wild-type and day 0 RNAi cells, to ~4 for day 2 RNAi cells, to over 9 for days 3, 4, or 5 RNAi cells (histograms in Fig. 4A). The accumulation of these bright spots was not Mitotracker-specific; we observed similar intensely staining regions in RNAi cells stained with another membrane potential-dependent dye, tetramethylrhodamine ethyl ester (250 nM) (J.L. Guler, unpubl.). In addition, if trypanosomes were treated with the respiratory uncoupler carbonylcyanide m-chlorophenylhydrazone (CCCP, 100 μM) (Fig. 4B, ±RNAi, panels 2 and 3), which dissipates membrane potential, fluorescence intensity of Mitotracker bright spots decreased to a level below that in either uninduced or induced RNAi cells without CCCP treatment (± RNAi, panel 1). Some lightly staining spots persist in CCCP-treated ACP RNAi cells (panel 2). However, these spots were further dissipated by 100 μM CCCP when a lower concentration (5 nM) of Mitotracker was used (panel 3). From these observations, we conclude that Mitotracker bright spots are at least partially due to localized regions of elevated membrane potential.

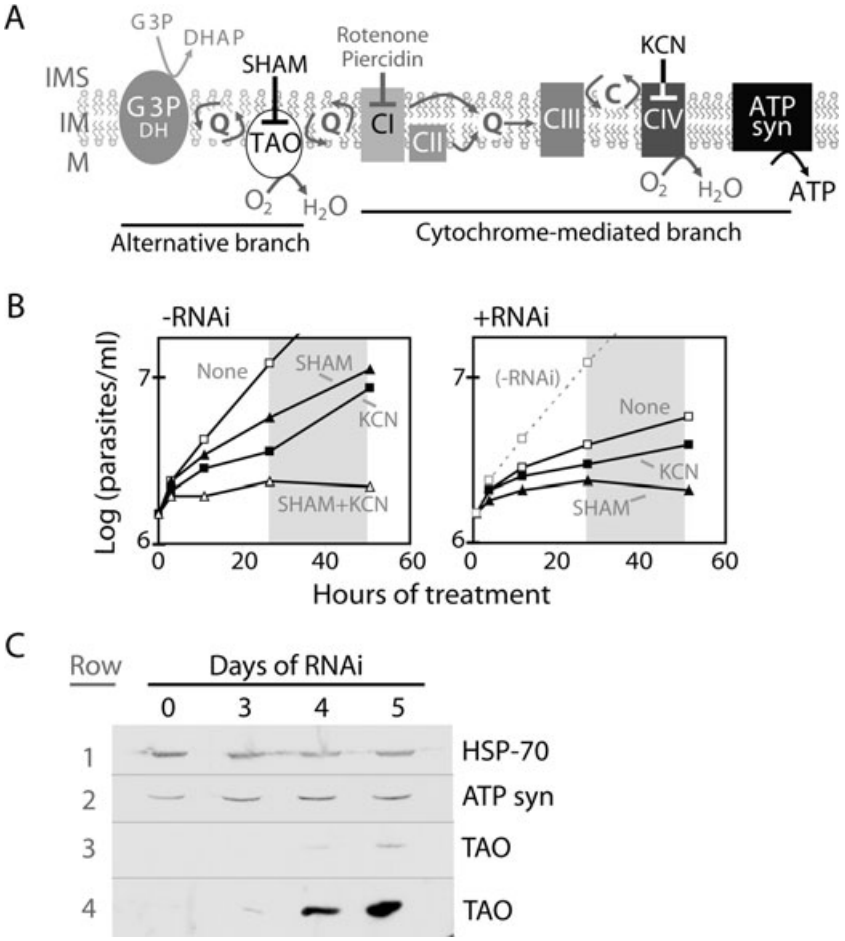

Fig. 3. Effect of ACP RNAi on the two branches of the *T. brucei* respiratory chain.
A. Schematic of the alternative and cytochrome-mediated branches of respiratory chain showing their respective inhibitors. IMS, intermembrane space; IM, inner membrane; M, matrix; G3PDH, glycerol-3-phosphate dehydrogenase; G3P, glycerol-3-phosphate; DHAP, dihydroxyacetone phosphate; Q, ubiquinone; TAO, trypanosome alternative oxidase; SHAM, salicylhydroxamic acid; CI, complex I (NADH-dehydrogenase); CII, complex II (succinate dehydrogenase); CIII, complex III (cytochrome *c* reductase); C, cytochrome *c*; CIV, complex IV (cytochrome *c* oxidase). In addition to CI and G3PDH, alternative NADH dehydrogenases may also contribute to the pool of reduced Q.
B. To show the contribution of each respiratory branch to trypanosome growth, uninduced RNAi cells (–RNAi, left panel) either were left untreated (except for an equivalent volume of ethanol, none) or were treated with 1 mM (final concentration) salicylhydroxamic acid (SHAM, ICN Biochemicals, 500 mM stock solution in ethanol), 1 mM KCN (Mallinckrodt Chemical Works, 500 mM stock solution in de-ionized water), or both SHAM and KCN. The final percentage of ethanol [< 1% (v/v)] had no effect on trypanosome growth. Cells induced for RNAi (+RNAi, right panel) were similarly left untreated (none) or treated with 1 mM SHAM or 1 mM KCN. The growth curve of uninduced RNAi (–RNAi) cells (dashed line) from the left panel is shown for comparison. The last time point in this line has been left out in order to truncate the height of the graph (value, 2.4×10^7 parasites ml^{-1}). Parasites per ml (*y*-axis) was calculated by multiplying cell density and dilution factor. ACP RNAi was induced with tetracycline 48 h prior to addition of drugs (SHAM or KCN) at 0 h. Growth rates (see *Results*) were calculated using cell densities between 26.5 and 50.5 h of treatment (grey region), with the assumption that growth is exponential during that period.
C. Effect of RNAi on levels of mitochondrial proteins as determined by Western blot. Proteins were HSP-70 (70 kDa, row 1), the F1β subunit of ATP synthase (55.7 kDa, row 2) and trypanosome alternative oxidase (TAO, 38 kDa, rows 3 and 4). Proteins in rows 1–3 were detected by the Enhanced Chemiluminescence assay and that in lane 4 by the much more sensitive assay (Supersignal West Femto, Pierce). Small regions of each blot are shown as no other major bands were detected.

ACP RNAi changes mitochondrial structure

To explain the alteration in Mitotracker staining (Fig. 4), we hypothesized that RNAi causes a change in mitochondrial structure. Transmission electron microscopy (EM) of cells after 5 days of RNAi showed that the mitochondrion in these cells was enlarged and had lower electron density (Fig. 5B) when compared with the mitochondrion in uninduced cells (Fig. 5A). In addition, large electron-dense aggregates (Fig. 5B, black arrowheads) and membranous bodies (asterisk '*'), which may be disrupted cristae, appeared only after RNAi. As these ultrastructural features were observed regardless of the fixation method or resin used (see *Experimental procedures*), the possibility of artifacts caused by improper fixation or suboptimal osmolarity can be ruled out. All other cellular structures,

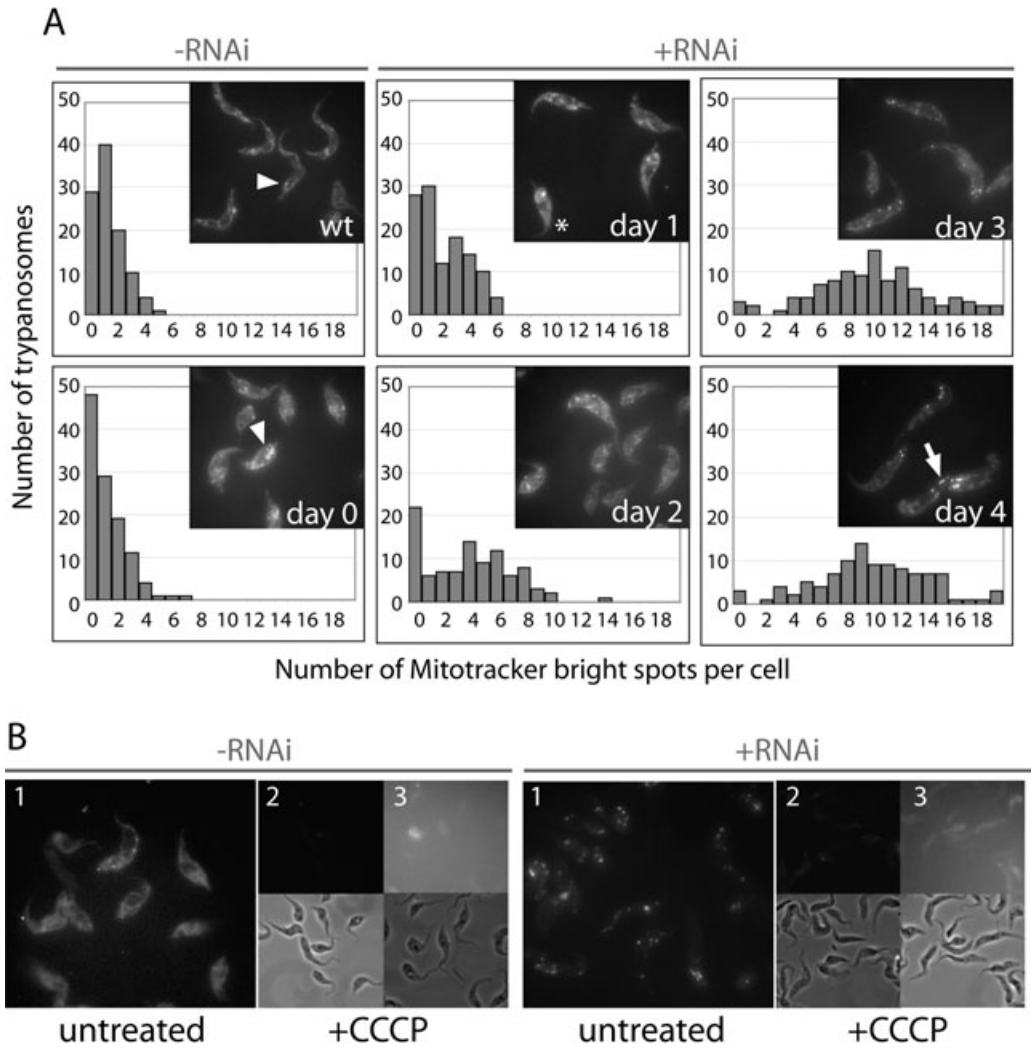

Fig. 4. Effect of ACP RNAi on the Mitotracker staining pattern.
A. Frequency histograms showing the distribution of cells with Mitotracker bright spots before (–RNAi) and after (+RNAi) induction of ACP RNAi. Inset fluorescence images show examples of Mitotracker staining patterns seen in each condition. Arrowhead, Mitotracker bright spots which are less common in wild-type or uninduced RNAi cells. Asterisk, normal Mitotracker staining in ACP RNAi cells. Arrow, larger Mitotracker bright spots in late stage RNAi cells (day 4).
B. Effect of CCCP on Mitotracker staining of uninduced (–RNAi) and induced (+RNAi, 4 days) trypanosomes. Panel 1, 40 nM Mitotracker (untreated with CCCP, 0.1 s exposure time). Panel 2, 40 nM Mitotracker (treated with 100 μM CCCP, 0.1 s exposure time). Panel 3, 5 nM Mitotracker (treated with 100 μM CCCP, 1 s exposure time). Mitotracker staining (top), phase images (bottom).

including the nucleus, acidocalcisomes, lipid droplets, endoplasmic reticulum (ER), flagellum and kinetoplast, appear to be normal following ACP RNAi (Fig. 5B). Fluorescence microscopy of the mitochondrial matrix protein, HSP-70, showed that enlargement of the mitochondrion began as early as 3 days after RNAi induction (Fig. 5D).

The presence of functional respiratory complexes within the membraneous bodies (asterisk '*' in Fig. 5B) could explain the Mitotracker bright spots we observed following RNAi. Immunofluorescence using antibodies against subunits of complexes III and IV, which normally pump protons, and complex V, which can work in reverse and hydrolyze ATP to generate a membrane potential (Schnaufer *et al.*, 2005; Brown *et al.*, 2006), showed that these complexes occasionally colocalize with the Mitotracker bright spots in RNAi cells (Fig. 6, white arrows). Not all mitochondrial proteins displayed this pattern; in fact, the mitochondrial matrix protein HSP-70 seemed to be excluded from the Mitotracker spots (Fig. 6, HSP-70, Z1 versus Z2).

ACP RNAi affects mitochondrial phospholipids

The decrease in respiration and the alteration in mitochondrial structure observed upon ACP RNAi could be

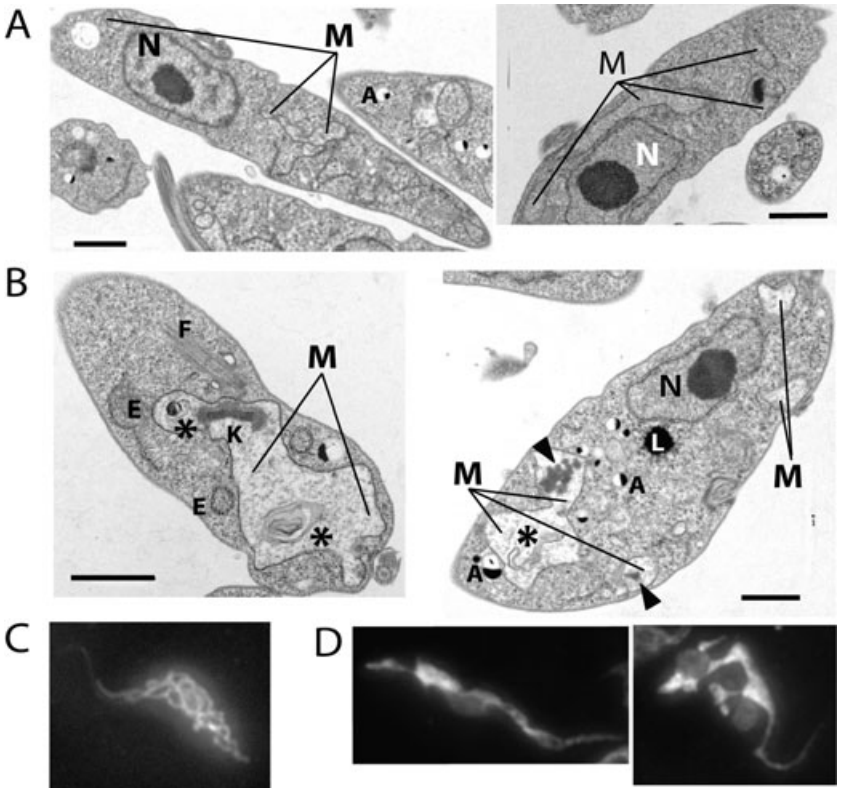

Fig. 5. Effect of ACP RNAi on mitochondrial ultrastructure. Transmission electron micrographs taken before (A) and after 5 days of ACP RNAi (B). Asterisk, membranous bodies; black arrowhead, protein aggregates; N, nucleus; M, mitochondrion; K, kinetoplast; A, acidocalcisome; L, lipid droplet; E, endoplasmic reticulum; F, flagellum. Fluorescence microscopy of cells probed for HSP-70 before (C) and after 3 days (left panel) or 4 days (right panel) of ACP RNAi (D).

explained by a change in mitochondrial membrane composition. As an initial test of this possibility, we cultured PCF trypanosomes in the presence of [^{14}C]threonine. This amino acid is taken up by cells and catabolized within the mitochondrion to form the fatty acid precursor, [^{14}C]acetyl-CoA. As in previous studies (Stephens *et al.*, 2007), ACP RNAi did not have a strong effect on threonine uptake or labelling of most phospholipids. However, RNAi caused some subtle changes in phospholipids such as phosphatidylethanolamine (GPEth[1]) and phosphatidylinositol (GPIno) (Fig. 7, Thr) that we subsequently confirmed in more rigorous experiments involving electrospray mass spectrometry (ES-MS) and gas chromatography-mass spectrometry (GC-MS).

Electrospray mass spectrometry was used to evaluate the effect of ACP RNAi on individual phospholipid species. We found that survey scans of whole-cell extracts revealed no significant changes attributable to RNAi. These studies were conducted both in the positive ion mode for detection of phosphatidylcholine (GPCho) and sphingomyelin (SM), and in the negative ion mode for detection of GPIno, GPEth, phosphatidylserine (GPSer), phosphatidylglycerol (GPGro), phosphatidic acid (GPA) and cardiolipin (T.K. Smith, unpubl.). However, further investigation of the individual phospholipid classes by parent ion scanning ES-MS/MS showed significant differences in the parent species of the collision-induced inositol-1,2-cyclic phosphate daughter ion (241 m/z), i.e. GPIno and inositolphosphoceramide (IPC) (Fig. 8A). The major diacyl-GPIno species (C18:0/C18:2, 861 m/z) decreased relative to the level of the major IPC species (34:1, 778 m/z). In addition, quantification of inositol containing phospholipids by GC-MS displayed a ~50% decrease in GPIno as early as 1 day after RNAi induction. This effect lasted for an additional 7 days, after which cells resistant to RNAi generally begin to overtake the population (Stephens *et al.*, 2007). Total IPC levels, on the other hand, remained constant throughout 8 days of RNAi (Fig. 8B).

We next investigated the effect of RNAi (4 days) on phospholipid species in mitochondria isolated from trypanosomes. While we did not observe significant differences between phospholipids from uninduced and induced cells when using the positive ion mode (Fig. S1A), we did detect changes in the negative ion mode (Fig. S1B). Further investigation of the individual phospholipid classes by parent ion scanning ES-MS/MS revealed a reduction in GPIno while the two major IPC species remained unchanged (Fig. 9A). In addition, we detected changes in parent species forming the collision-induced daughter ion (m/z 196) characteristic of GPEth

[1]The lipid nomenclature used in this paper follows the most recent standards developed by an international consortium (Fahy *et al.*, 2005).

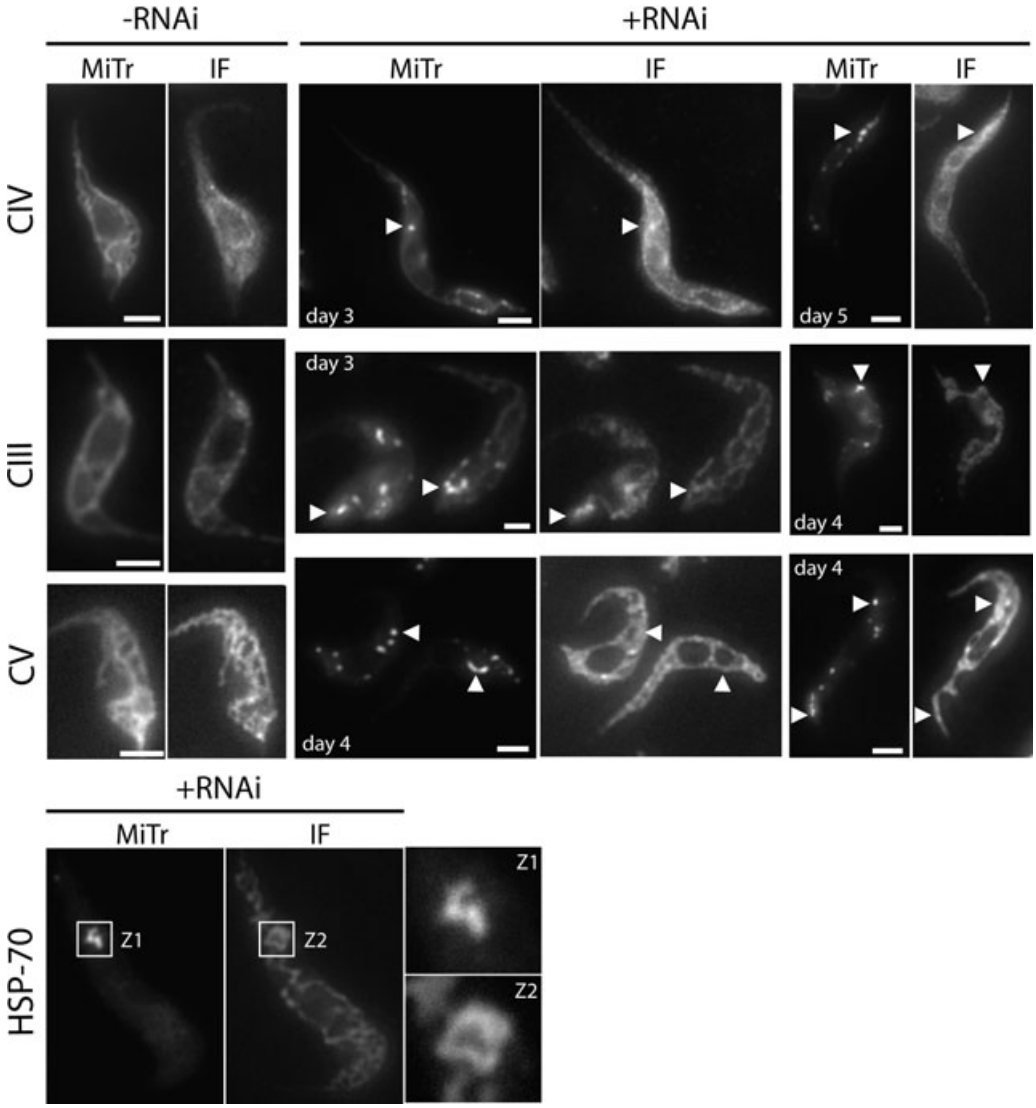

Fig. 6. Distribution of respiratory complexes in relation to Mitotracker bright spots. Mitotracker staining (MiTr) and immunofluorescence (IF) of respiratory complex IV (CIV, cytochrome *c* oxidase subunit IV), complex III (CIII, cytochrome *c* reductase iron sulphur protein subunit), ATP synthase (ATP syn, F1β subunit) and HSP-70 (mitochondrial matrix chaperone). Arrowheads indicate points of colocalization between Mitotracker bright spots and subunits of respiratory complexes. In the HSP-70 panel, boxes indicate zoomed regions (Z1 and Z2) shown in the right-hand panels.

and plasmenyl-GPEth (Fig. 9B). The major diacyl-GPEth species (C18:0/C18:2, 739 m/z) was reduced considerably, along with other minor diacyl species, while the plasmenyl-GPEth species [(E) C16:0/C18:2 and C18:0/C18:2, 699 and 726 m/z respectively] remained unchanged. As in whole cells, parent ion scanning revealed no RNAi-mediated changes in mitochondrial GPCho, SM and GPSer (Fig. S2A and B). Additionally, parent ion scanning ES-MS/MS of 153 m/z indicative of glycerophospholipids, including GPA and GPGro, showed no significant changes including those for cardiolipin, whose [M-2H]2– doubly charged ion is observed at 748 m/z (Fig. S2C), along with the [M-H]– ion at 1498 m/z (Fig. S3A). As cardiolipin has not been described in trypanosomes prior to this report, further analysis by accurate MS revealed four main cardiolipin species (T.K. Smith, unpubl.). Daughter ion ES-MS/MS fragmentation of one of the cardiolipin species (1500 m/z) revealed two GPA daughter ions of the cardiolipin (linked by a glycerol) as 1,2-O-(C18:2)acyl,(C18:0)acyl glycerol-3-*P* (m/z 699) and 1,2-O-(C18:2)acyl,(C22:6)acyl glycerol-3-*P* (m/z 743) (Fig. S3C). Fragmentation of these two ion species are depicted in Fig. S3C, which correspond to the daughter ions observed in Fig. S3B. Full lipid profiling on the mitochondrial lipids, including the cardiolipins will be published elsewhere (T.K. Smith and J.L. Guler, in preparation).

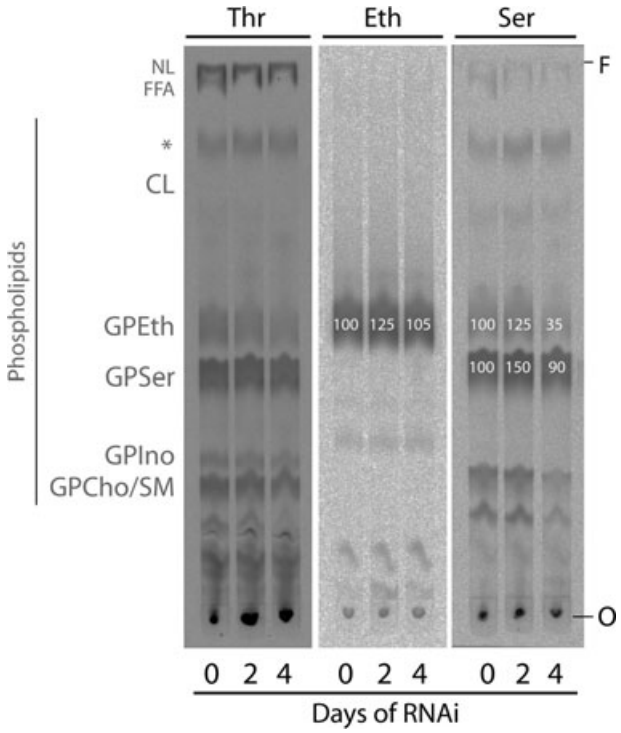

Fig. 7. Effect of ACP RNAi on newly synthesized phospholipids. Cells were metabolically labelled with either [^{14}C]threonine (Thr), [^{14}C]ethanolamine (Eth), or [^{14}C]serine (Ser) after 0, 2, or 4 days of ACP RNAi. Extracted lipids were fractionated by thin layer chromatography and detected by autoradiography (~10^8 cell equivalents per lane). Positions of phospholipid standards are shown [neutral lipids (NL), free fatty acids (FFA) and phospholipids (CL, cardiolipin; GPEth, phosphatidylethanolamine; GPSer; phosphatidylserine; GPIno, phosphatidylinositol; GPCho, phosphatidylcholine; SM, sphingomyelin]. White numbers on TLC bands represent percentage of phospholipid levels (uninduced cells were set to 100%) as quantified from the phosphorimager exposure. Each panel was exposed to the phosphorimager screen for an optimized time; Thr (4 days), Eth (6 h), Ser (18 h). Asterisk, unknown band that could possibly be trypanosome cardiolipin. F, solvent front. O, sample origin.

To further evaluate the RNAi-mediated loss of GPEth in isolated mitochondria, we investigated the two main pathways responsible for its synthesis; the Kennedy pathway utilizes cytidine diphosphate (CDP)-ethanolamine and diacylglycerol (DAG) substrates in the ER and GPSer decarboxylation takes place on the inner mitochondrial membrane (Voelker, 1997). Although we have not been able to measure activity of GPSer decarboxylase directly (T.K. Smith, unpubl.), metabolic labelling with [^{14}C]ethanolamine (which labels GPEth made by the ER pathway) or [^{14}C]serine (which labels GPEth made by the mitochondrial pathway) allowed us to determine which of the two pathways was inhibited during ACP RNAi. We found that [^{14}C]ethanolamine incorporation into GPEth did not decrease (Fig. 7, Eth), indicating that the Kennedy pathway remains fully functional following the loss of ACP. In contrast, [^{14}C]serine incorporation into GPEth (presumably via GPSer decarboxylation, see below) decreased to ~35% of uninduced levels following 4 days of ACP RNAi and [^{14}C]serine-labelled GPSer levels increased to ~150% of uninduced levels after 2 days but then return to normal levels following 4 days of RNAi (Fig. 7, Ser). In these experiments it is likely that radiolabel from [^{14}C]serine incorporates mostly into the head-groups of GPSer and GPEth rather than into the acyl chains of these phospholipids. The latter could occur if [^{14}C]serine was converted to [^{14}C]acetyl-CoA through the sequential action of serine dehydratase (which converts serine to pyruvate) and pyruvate dehydrogenase; the [^{14}C]acetyl-CoA could then be incorporated into newly synthesized fatty acids. Unpublished experiments (by T.K. Smith) with [^{14}C]serine labelling of wild-type procyclic trypanosomes indicate that this is not the case. Furthermore, if this were occurring in significant amounts, we would expect other phospholipids labelled in the serine experiment to decrease by amounts comparable to that of GPEth [which is not apparent following 2 or 4 days of ACP RNAi (Fig. 7, Ser)].

Discussion

Our current studies, which evaluate the consequences of RNAi knock-down of ACP, build on our previous report that the *T. brucei* mitochondrial fatty acid synthase makes saturated fatty acids with the longest being palmitate (C16) (Stephens *et al.*, 2007). Effects such as respiratory inhibition (Figs 1 and 2, Table 1), alteration of mitochondrial ultrastructure (Fig. 5), and changes in phospholipid composition (Figs 7,8 and 9) following ACP RNAi indicated these fatty acid products are required to preserve proper mitochondrial function. We also found with BSF trypanosomes (but not with PCFs) that knock-out of ACP caused loss of the mitochondrial genome (A.M. Clayton, J.L. Guler, M.E. Lindsay and P.T. Englund, in preparation). Some of these effects must be secondary, and to evaluate which is the primary consequence of ACP depletion, we assessed the timing of appearance of each effect following ACP knock-down [ACP protein levels were down by 75% after just 1 day of RNAi (Stephens *et al.*, 2007)]. We found that respiratory defects and alterations in Mitotracker staining were not prominent until 2–3 days of RNAi (Figs 1 and 4A) and enlarged mitochondria did not become prevalent until after 3–4 days (Fig. 5D). The earliest detectable effects were on phospholipid levels; GPIno was reduced by ~50% after just 1 day (Fig. 8B) and GPSer was increased ~50% after 2 days (Fig. 7, Ser). Although the changes in phospholipid levels will be addressed later, these kinetic data are consistent with the possibility that the primary effect of ACP RNAi is on phospholipid composition.

In the first step in our investigation, we found that ACP RNAi caused a reduction in O_2 consumption (Fig. 1).

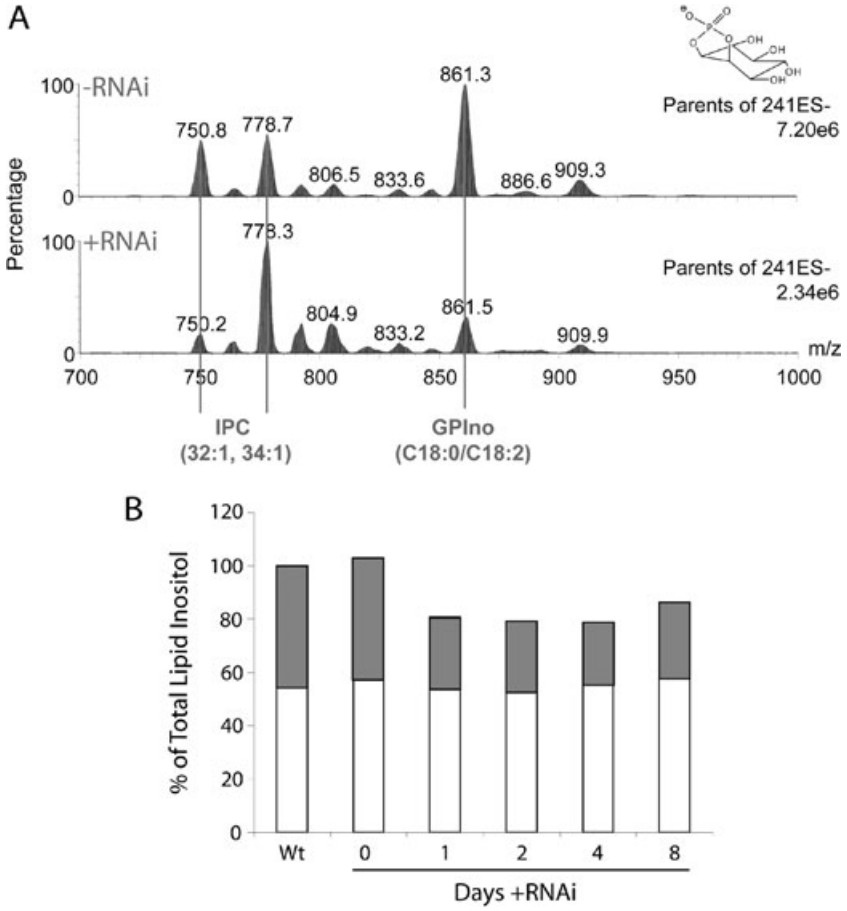

Fig. 8. Effect of ACP RNAi on inositol-containing phospholipids from whole cells.
A. Lipids extracted from whole trypanosomes either uninduced (–RNAi) or induced for RNAi for 4 days (+RNAi) were analysed by ES-MS/MS for GPIno and IPC phospholipids (parent ion scanning of m/z 241). Peak assignments are based on MS/MS daughter ion spectra and comparisons to previous experiments (G.R. Richmond and T.K. Smith, unpubl. data).
B. Lipid *myo*-inositol levels were quantified by GC-MS from whole wild-type cells (wt), uninduced RNAi cells (day 0), or cells induced for RNAi for various days. Values of *myo*-inositol are the mean of three separate analyses (standard deviation for any triplicate was not greater than 7%) and have been normalized to wild-type levels (wt, set to 100%, 126 pmol total *myo*-inositol per 1×10^5 cell equivalents: GPIno (grey bar), 68.5 pmol; IPC (white bar), 57.9 pmol).

Because of our previous finding that *T. brucei* mitochondrial fatty acid synthesis also supplies the octanoate precursor for synthesis of lipoic acid (Stephens *et al.*, 2007), we considered whether a decrease in lipoic acid content alone could cause the drastic effects on cell growth and respiration observed during ACP RNAi (Fig. 1). Pyruvate dehydrogenase and α-ketoglutarate dehydrogenase, two lipoic acid-dependant enzymes, contribute to the pool of mitochondrial NADH and thus, complex I activity. Although a decrease in the activity of these two enzymes could theoretically account for the observed respiratory defects displayed in Fig. 1, there are reasons why this is probably not the case. First, RNAi knock-down of either dehydrogenase does not cause any dramatic effects on trypanosome growth (Bochud-Allemann and Schneider, 2002), and second, decreases in activity of other respiratory complexes (Table 1) easily account for the respiratory defect.

In fact, based on the inhibition of complexes II, III and IV (Table 1 and Fig. 2B) and decreased sensitivity to KCN (Fig. 3B), we concluded that the respiratory effects of ACP RNAi are confined predominantly to the cytochrome-mediated branch rather than the alternative branch. In addition, the RNAi-mediated increase in SHAM sensitivity (Fig. 3B) and TAO protein levels (Fig. 3C) mirror effects seen after RNAi-depletion of complexes III and IV (Horváth *et al.*, 2005) and increases in oxidative stress (Fang and Beattie, 2003b). Thus, upregulation of the alternative pathway must be an attempt to compensate for the loss of conventional respiration by oxidizing excess reducing equivalents that build up downstream of ubiquinone (see Fig. 3A) and thereby prevent an increase in production of reactive oxygen species (ROS) (Fang and Beattie, 2003b). However, we found that generation of ROS increases sixfold after 2 days and > 60-fold after 4 days of RNAi (as measured by flow cytometry following staining with 2′,7′-dichlorodihydrofluorescein diacetate [1 μM (Fang and Beattie, 2003b; Figarella *et al.*, 2006)], J. L. Guler, unpubl.), indicating that TAO, although upregulated, is still unable to divert all electron transport from the cytochrome-mediated pathway. The resulting oxidative stress could contribute to the RNAi-mediated enlargement of the mitochondrion (Fig. 5B) (for review see Wakabayashi, 2002).

As discussed previously, it is uncertain whether complex I even exists in *T. brucei*. If our in-gel and spectrophotometric assays are actually detecting a *bona fide* complex I, the absence of a strong RNAi-mediated effect

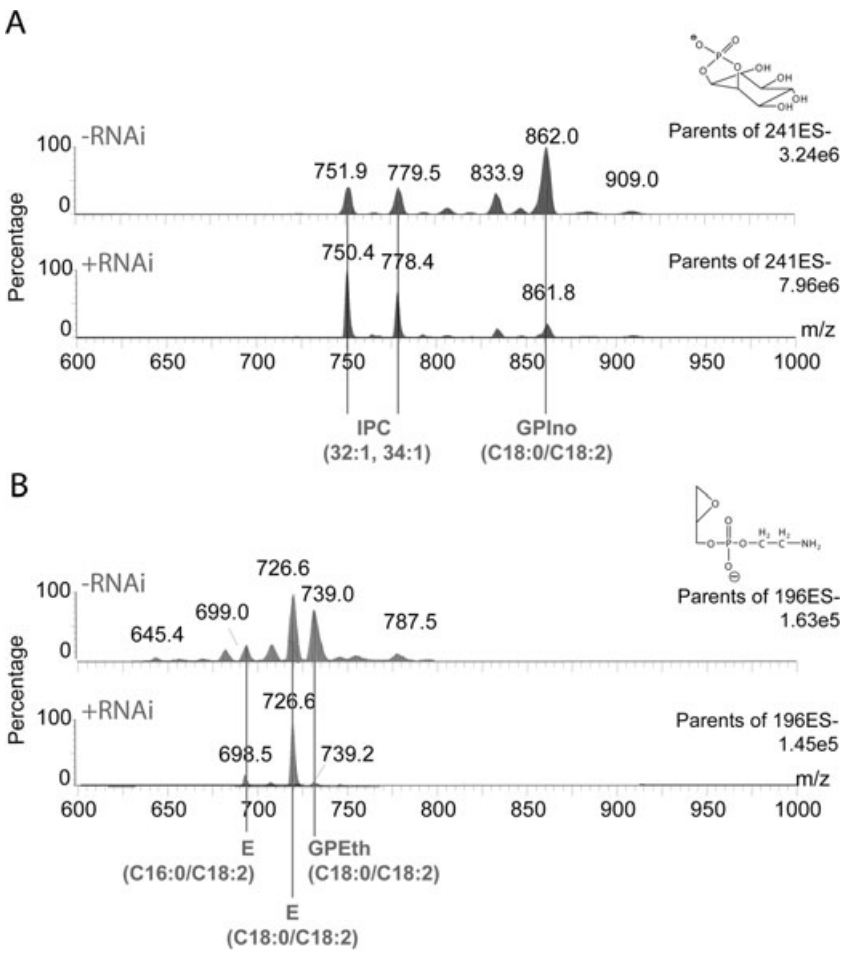

Fig. 9. Effect of ACP RNAi on inositol- and ethanolamine-containing phospholipids from mitochondria. Mitochondria were purified and lipids were extracted from uninduced (–RNAi) and induced ACP RNAi cells (+RNAi, 4 days) and analysed by ES-MS/MS for either (A) GPIno and IPC phospholipids [parent ion scanning of the m/z 241 fragment (see structure)] or (B) GPEth phospholipids [parent ion scanning of the m/z 196 fragment (see structure)]. Peak assignments are based on MS/MS daughter ion spectra and comparisons to previous experiments on whole-cell extracts (G.R. Richmond and T.K. Smith, unpubl. data). E, plasmenyl (alkenylacyl) phosphatidylethanolamine.

would indicate that ACP does not play an essential structural or functional role in complex I as it does in fungi (Schneider *et al*., 1997) and mammals (Runswick *et al*., 1991; Cronan *et al*., 2005). However, the reliability of this conclusion is limited by the observation that in-gel activity was not inhibited by piericidin (5 μM) or rotenone (10 μM) (A. Horváth and P. Čermáková, pers. comm.), two specific inhibitors of complex I in other organisms. However, resistance to these drugs could be explained if *T. brucei* complex I is highly diverged and lacks the appropriate binding sites for these inhibitors.

While complexes I and V were relatively unaffected by ACP RNAi (Table 1), it appears that the activity, or perhaps the assembly, of complexes II, III and IV are especially sensitive to changes in levels of fatty acids or other downstream products of the mitochondrial synthase. One possibility is that ACP RNAi affects synthesis or repair of cardiolipin, a mitochondrial phospholipid that is especially important for respiratory complex assembly (for review see Li *et al*., 2007). However, using ES-MS, we detected no significant changes in cardiolipin following RNAi (Fig. S3). Another possibility is that inactivation of respiratory complexes is due to the accumulation of lysophospholipids as observed in ACP-depleted *Neurospora crassa* (Schneider *et al*., 1995). Lysophospholipids are produced when phospholipases remove acyl chains that have been damaged by ROS (for review see Nigam and Schewe, 2000). Presumably, these highly reactive repair intermediates could be reacylated using fatty acids synthesized in the mitochondrion. However, we detected no increase in lysophospholipids by ES-MS (T.K. Smith, unpubl.), a finding similar to that from *S. cerevisiae* mitochondrial ACP mutants (Schneider *et al*., 1995).

Changes in other phospholipids were detected following ACP RNAi (Figs 8 and 9). While GPIno was decreased in extracts of both whole cells and isolated mitochondria, GPEth was decreased only in isolated mitochondria. This latter result indicates that the global decline in GPIno is not solely due to the decrease in mitochondrial levels because mitochondrial phospholipids make up a small fraction of total phospholipids. Furthermore, it is likely that these effects are dependent on the depletion of ACP and not due to a decrease in growth rate or viability during the induction. For example, mutants defective in an enzyme essential for *de novo* synthesis of *myo*-inositol have a

growth defect but do not display significant changes in levels of GPIno or GPEth (Martin and Smith, 2006).

How can ACP RNAi cause a decrease in extra-mitochondrial GPIno? This phospholipid is the third most abundant phospholipid in PCF trypanosomes (Patnaik *et al*., 1993) and consequences of its decrease could be diminished by the presence of another inositol-containing phospholipid, IPC, whose total levels remain unchanged after RNAi (Fig. 8B). Therefore, it is possible that CDP-DAG (the precursor for synthesis not only of GPIno, but also GPSer, GPGro and cardiolipin) could be directed away from GPIno synthesis and towards synthesis of other phospholipids, such as cardiolipin, which are especially sensitive to ROS damage (Edman and Ericson, 1987; Schlame *et al*., 1993). In addition, changes in phospholipid content may disrupt formation of mitochondrial-associated membranes (MAMs), a subcompartment of the ER that facilitates phospholipid transfer to and from the mitochondria and one site of GPIno synthesis (Gaigg *et al*., 1995). Although likely a secondary consequence, a decrease in activity of the MAM-localized GPIno synthase could further diminish GPIno levels.

GPEth, which is also abundant in trypanosomes (Doering *et al*., 1993; Patnaik *et al*., 1993), contributes to maintenance of topology (Zhang *et al*., 2005), translocation (Rietveld *et al*., 1995; Mikhaleva *et al*., 2001), and folding of *E. coli* membrane proteins (Bogdanov *et al*., 1996; Bogdanov and Dowhan, 1999). In addition, GPEth appears to be critical for optimal activity of respiratory complexes (Schagger *et al*., 1990; Birner *et al*., 2001) and proper ubiquinone function (Mileykovskaya and Dowhan, 1993). In fact, the synthetic lethality of yeast mitochondrial GPEth and cardiolipin synthesis mutants (Gohil *et al*., 2005) suggests that mitochondrial GPEth may have a function similar to cardiolipin (Li *et al*., 2007).

The importance of GPEth is emphasized by the fact that there are at least two pathways responsible for its synthesis: the Kennedy pathway (generally in the ER) and GPSer decarboxylation (generally in the mitochondrion). In some organisms, there are additional sites of GPSer decarboxylation (Nerlich *et al*., 2007), but trypanosomes resemble mammals (Kuge *et al*., 1991) in that they have a single gene for GPSer decarboxylase whose product is predicted to be mitochondrial (http://www.genedb.org/genedb/tryp). The relative flux through the two pathways varies in different cell types and depends on availability of substrates (Bleijerveld *et al*., 2007). In *T. brucei*, we were not able to measure the contribution of each pathway owing to uncertainty concerning the intracellular pool size of non-radioactive ethanolamine and serine. Labelling with [^{14}C]ethanolamine, which is converted to GPEth in the ER, is a control to assess general phospholipid synthesis during ACP RNAi (Fig. 7, Eth). During [^{14}C]serine labelling, the initial increase in GPSer (day 2) and subsequent decrease in GPEth (day 4) demonstrated the selective inhibition of ACP RNAi on the mitochondrial pathway (Fig. 7, Ser). At this point, however, we cannot tell whether this is due to inhibition of GPSer transport to mitochondria (possibly through the disruption of MAMs, see above) or inhibition of GPSer decarboxylase itself (possibly through the disturbance of the inner mitochondrial membrane, see below). Interestingly, decreases in mitochondrial GPEth in GPSer decarboxylase mutants cause rounding and fragmentation of mammalian mitochondria (Steenbergen *et al*., 2005) which along with oxidative stress (mentioned above), could explain the abnormal mitochondrial morphology seen during ACP depletion (Fig. 5B and D).

The enlargement of the mitochondrion was preceded by the appearance of Mitotracker bright spots, which, based on CCCP experiments (Fig. 4B), are at least partially due to localized regions of elevated membrane potential. EM and immunofluorescence experiments in Figs 5 and 6 provide evidence that these bright spots are not a result of massive fragmentation of the mitochondrion. One potential scenario, however, is that RNAi induced vesiculation of the inner membrane. Perhaps these vesicles, which may correspond to the membranous bodies detected by EM (Fig. 5B), can actively generate a membrane potential because they contain normal levels of GPEth whereas this phospholipid is depleted from other parts of the inner membrane. Another possibility is that the remaining GPEth is sequestered in distinct regions of the inner membrane which creates microenvironments where respiration and thus, production of membrane potential occur at a higher rate. Whatever the case, we cannot rule out the possibility that the entire inner membrane is generating a membrane potential that is below the limits of our detection with Mitotracker.

Although beyond the scope of this paper, the reductions in GPIno and GPEth could also have detrimental effects on glycosylphosphatidylinositol (GPI) biosynthesis. GPIno provides the anchoring hydrophobic moiety of the GPI (Masterson *et al*., 1989) and GPEth donates phosphoethanolamine (Menon *et al*., 1993). As GPIno and GPEth levels are also decreased after ACP knockout in BSF trypanosomes (T.K. Smith, unpubl.), a drug targeting mitochondrial fatty acid synthesis could indirectly diminish the BSFs ability to evade the host immune system through a detrimental effect on GPI anchor biosynthesis required for cell surface expression of the variant surface glycoprotein (Nagamune *et al*., 2000; Chang *et al*., 2002; Smith *et al*., 2004).

There are several classical inhibitors that target fatty acid synthesis, some of which have been tested on trypanosomes with varying efficacies (Morita *et al*., 2000; Paul *et al*., 2004; Jones *et al*., 2005). In addition, new inhibitors of fatty acid synthesis are still being developed

(Ondeyka *et al*., 2006; Wang *et al*., 2006). One such class of inhibitors, the pantothenamides, mimics pantothenate, a vitamin required for coenzyme A biosynthesis, and consequently, ACP biosynthesis (Zhang *et al*., 2004). We found that pantothenamides effectively kill both PCF and BSF *T. brucei*, although the EC_{50}'s are high [~130 and ~75 μM respectively (J.L. Guler, unpubl. data)]. Based on metabolic labelling of fatty acids with [^{14}C]threonine and [^{14}C]pyruvate and detection of protein lipoylation by Western blot analysis (as described in Stephens *et al*., 2007), we found that these compounds target trypanosomal mitochondrial fatty acid synthesis. Pantothenamides may also affect the ELO pathway, which is responsible for bulk fatty acid synthesis within these cells.

In conclusion, our studies demonstrate the extent to which the trypanosome relies on mitochondrial fatty acid synthesis. Loss of this pathway affects respiration, organellar morphology and, in the BSF, maintenance of the mitochondrial genome (J.L. Guler, in preparation). One objective of this paper was to explain how knockdown of mitochondrial fatty acid synthesis could bring about these varied effects. While the chain of events leading to all these phenotypes is obviously complex, we present strong evidence that the primary effect of ACP RNAi is on phospholipid composition. Even though we could not detect phospholipid repair intermediates in RNAi cells, a decrease in levels of mitochondrial acyl-ACPs could potentially lead to the inhibition of local phospholipid repair. Thus, in order to maintain normal levels of cardiolipin in RNAi mitochondria (as described above), CDP-DAG may be directed away from production of abundant/redundant phospholipids such as GPIno and towards synthesis of cardiolipin precursors. We hypothesize that this change in phospholipid content disrupts membrane subcompartments such as MAMs and the inner mitochondrial membrane which may normally require a specific repertoire of phospholipids for proper functioning. This disruption could contribute to the decrease in mitochondrial GPEth through interruption of GPSer transport or inhibition of GPSer decarboxylase; it could also cause further decreases in GPIno through inhibition of GPIno synthase. Future studies on mitochondrial fatty acid synthesis should clarify these individual events.

Experimental procedures

Trypanosomes

Wild-type PCF trypanosomes were *T. brucei* strain 29–13. Strains constructed for tetracycline-inducible RNAi of ACP (Stephens *et al*., 2007) and ODC (Wang *et al*., 2000) utilized the pZJM vector (Wang *et al*., 2000) transfected into strain 29–13. All PCF trypanosomes were maintained at 28°C and 5% CO_2 in SDM-79 medium (Brun and Schonenberger, 1979) supplemented with 10% fetal bovine serum and antibiotics as needed (15 μg ml^{-1} G418, 50 μg ml^{-1} hygromycin, 2.5 μg ml^{-1} phleomycin). RNAi was induced with 1 μg ml^{-1} tetracycline. Cell densities were monitored using a Coulter cell counter (model Z1, Coulter).

Oxygen electrode measurements

O_2 consumption of PCF trypanosomes was measured essentially as previously described (Beattie *et al*., 1994). Briefly, after harvest, cells (~9×10^7 cells, containing ~1 mg of protein) were washed (150 mM NaCl, 5 mM glucose and 20 mM sodium phosphate, pH 7.9) and then suspended in assay buffer (125 mM sucrose, 65 mM KCl, 5 mM Hepes, pH 7.2, 1 mM $MgCl_2$, 2.5 mM potassium phosphate, 1 mM EDTA). Measurements on intact cells were performed at 28°C in a 2 ml chamber of a Clark-type O_2 electrode (Yellow Springs Instruments). No additional substrates were added.

Assays of respiratory complex activity

Mitochondrial vesicles (2×10^8 cell equivalents) were isolated and lysed with 2% dodecylmaltoside as described (Horváth *et al*., 2005). Activities of respiratory complexes I and IV were detected by in-gel assays following electrophoresis of mitochondrial lysate (80 μg of protein per lane) on a 2–15% blue native PAGE gel. To assay NADH dehydrogenase activity (complex I), the gel was incubated in 0.14 mM NADH and 1 mg ml^{-1} nitrotetrazolium blue chloride. The insoluble blue product precipitated in a region of the gel where putative *T. brucei* complex I has been shown to migrate (~650 kDa) (Horváth *et al*., 2005). To assay complex IV activity, the gel was incubated in 50 mM sodium phosphate, pH 7.4, 1 mg ml^{-1} 3,3′-diaminobenzidine, 24 U ml^{-1} catalase, 1 mg ml^{-1} cytochrome *c* and 75 mg ml^{-1} sucrose. The brown precipitate was observed in the same region of the gel as complex IV activity from *Leishmania tarentolae* mitochondria (Horváth *et al*., 2005; Zíková *et al*., 2006).

Activities of respiratory complexes I, III and IV were also measured spectrophotometrically in mitochondrial lysates as previously described (Horváth *et al*., 2005; Zíková *et al*., 2006). For NADH:ubiquinone oxidoreductase activity (which detects both complex I and alternative NADH dehydrogenases), mitochondrial lysate was incubated with NADH in the presence of KCN. Following the addition of an artificial electron acceptor (either ubiquinone 2 or ferricyanide) the reaction was measured by a decrease in A_{340}. For complexes III and IV activities, mitochondrial lysate was incubated with either reduced decylubiquinone and horse heart cytochrome *c* (complex III assay) or reduced cytochrome *c* alone (complex IV assay) and the reactions were followed at A_{550}. Complexes II and V activities were also assayed spectrophotometrically using the following methods. Complex II activity was measured in mitochondrial vesicles (5 μl; 40 μg of protein) preincubated for 10 min at 30°C in cuvettes containing 1 ml of assay buffer (25 mM potassium phosphate, pH 7.2, 5 mM $MgCl_2$ and 20 mM sodium succinate). Rotenone (2 μg ml^{-1}), antimycin A (2 μg ml^{-1}), KCN (2 mM) and ubiquinone 2 (65 μM) were then added and the activity of complex II was measured by following the reduction of 2,6-dichlorophenolindophenol (DCPIP; 50 μM) at A_{600} (assuming

an extinction coefficient of 19.1 $mmol^{-1}$ cm^{-1}). Complex V activity was measured in cuvettes containing 1 ml of ATPase assay buffer (50 mM Tris-HCl, pH 8.0, 1 mM ATP, 3 mM $MgCl_2$), 1 mM phosphoenolpyruvate, 1.1 μl of lactate dehydrogenase (type II from rabbit muscle, 1020 U mg^{-1} (12 240 U ml^{-1}), Sigma), 1 μl of pyruvate kinase [type VII from rabbit muscle, 378 U mg^{-1} (1852 U ml^{-1}), Sigma] and 5 μl of mitochondrial vesicles (40 μg of protein). The reaction was started with the addition of 0.3 mM NADH and followed by the decrease in A_{340}. As ATPase activity was sometimes lost after freezing and thawing, only fresh samples were assayed.

Western blots

All antibodies used for Western blots and immunofluorescence were made against *T. brucei* proteins unless otherwise noted. For Western blots, trypanosomes (~5×10^6 cells $lane^{-1}$) were harvested and stored at –80°C until fractionated by 10% or 12% SDS-PAGE. The proteins were then transferred to a PVDF membrane and incubated with either rabbit anti-*Crithidia fasciculata* HSP-70 [1:1000 (Effron *et al.*, 1993) and see note below], rabbit anti-ATP synthase F1 β-subunit [ATPsyn, 1:1000, provided by R. Benne (Speijer *et al.*, 1997)], or mouse anti-TAO [1:1000, provided by G.C. Hill (Chaudhuri *et al.*, 1998)] followed by the appropriate secondary antibody conjugated to horseradish peroxidase (HRP, Jackson Immunoresearch, 1:5000–10 000). HRP was detected by either the Enhanced Chemiluminescent Substrate kit (ECL, Amersham Biosciences) or the Supersignal West Femto kit (Femto, Pierce).

The HSP-70 antibody was made against a protein (likely an HSP-70) that was purified many years ago from a *Crithidia fasciculata* mitochondrial fraction. The antibody recognizes a 70 kDa polypeptide on Western blots of *T. brucei* total cell protein (Fig. 3C) and it colocalizes with Mitotracker staining in *T. brucei* wild-type cells (J.L. Guler, unpubl.)

Fluorescence and electron microscopy

For Mitotracker staining, cells were harvested and stained with 40 nM Mitotracker Red CMX-ROS (Molecular Probes) for 10 min at 27°C in SDM-79 medium followed by another 20 min in medium alone (Stephens *et al.*, 2007). After re-suspension in PBS, cells were fixed in 4% paraformaldehyde (Wang and Englund, 2001) and viewed on a Zeiss Axioscope Microscope or stained for immunofluorescence (see below). For quantification of the Mitotracker phenotype, the number of Mitotracker bright spots per cell was manually counted for ~100 trypanosomes (wild type and day 0 through day 4 of ACP RNAi). For uncoupler treatment, trypanosomes were incubated with fresh CCCP (carbonyl cyanide *m*-chlorophenylhydrazone, Sigma, 100 μM in DMSO) as previously described (Brown *et al.*, 2006) prior to Mitotracker staining (as above). For immunofluorescence, Mitotracker-stained fixed cells were incubated with the primary antibodies mentioned above [anti-ATPsyn (1:1000), anti-HSP-70 (1:200)] or rabbit anti-*Leishmania tarentolae* cytochrome *c* oxidase subunit IV [CIV, 1:100 (Maslov *et al.*, 2002)] and anticytochrome *c* reductase iron sulphur protein [CIII, 1:200 (McManus *et al.*, 2001)] followed by the appropriate AlexaFluor 488 secondary antibody (Molecular Probes) (diluted 1:500–1:1000) (Wang and Englund, 2001).

For transmission EM, cells were fixed in 2.5% (v/v) glutaraldehyde in either 0.1 M sodium cacodylate buffer, pH 7.4 or 0.1 M sodium phosphate buffer, pH 7.4, for 1 h at 4°C, and post-fixed with 2% osmium tetroxide in the same buffer for 1 h at room temperature. After dehydration the cells were embedded in either PolyBed (Polysciences) or Epon-Araldite (Serva) and sectioned. Thin sections were stained with lead citrate and uranyl acetate, and examined in a JEOL JEM 1010 microscope.

Phospholipid analysis using thin-layer chromatography

Trypanosomes were labelled in minimal media to enhance uptake of the radioactive compounds. This minimal medium, which lacks hemin and FBS, consists of Minimal Essential Medium (MEM, Gibco), the basal medium used for SDM-79, BME vitamins solution (Sigma) and SDM-79 solids (Brun and Schonenberger, 1979), leaving out either threonine or serine. Prior to labelling, trypanosomes (~1×10^8 cells in 1 ml) were incubated in this minimal medium at 28°C. After ~30 min, 1.2 μCi L-Threonine-UL-^{14}C hydrochloride (Sigma, 155 mCi $mmol^{-1}$) or 0.2 μCi Ethanolamine-1,2-^{14}C hydrochloride (Sigma, 13.8 mCi $mmol^{-1}$) was added and incubated at 28°C for another 2–4 h. Trypanosomes were also labelled with 1.2 μCi L-Serine-UL-^{14}C (Sigma, 127 mCi $mmol^{-1}$) for 2 h as above, washed twice in PBS, and then chased in normal SDM-79 medium for two additional hours. For phospholipid analysis, lipid species were extracted in 10:10:3 chloroform/methanol/water, dried under N_2 gas and re-suspended in chloroform before fractionation on thin layer chromatography (TLC) as previously described (Leray *et al.*, 1987). Briefly, TLC plates (Whatman LK5D) were pre-washed in 1:1 chloroform/methanol, air-dried, wet with 2.3% boric acid in ethanol and dried for 15 min in a 100°C oven. Standards and samples (20 μl) were loaded and plates were run in 30:35:7:35 chloroform/ethanol/water/triethylamine, dried and visualized by phosphorimaging. Non-radioactive standards (~50 μg each) were detected by phosphorimaging after spraying with primuline (50 μg ml^{-1} in 4:1 acetone/water), viewing under UV light and spotting with [^{14}C]butyrate.

Phospholipid analysis using electrospray mass spectrometry

Phospholipid analysis was performed on whole cells and isolated mitochondrial vesicles from PCF trypanosomes. For whole-cell analysis, ~$1–5 \times 10^8$ cells uninduced or induced for ACP RNAi for 4 days were harvested and washed in PBS. For mitochondrial analysis, mitochondrial vesicles from ~1×10^{10} trypanosomes, uninduced or induced for ACP RNAi for 4 days, were isolated on a 20–35% renografin gradient as reported previously (Braly *et al.*, 1974; Stephens *et al.*, 2007). Both types of samples were extracted according to the method of Bligh-Dyer (Bligh and Dyer, 1959), dried under N_2 and stored at 4°C until analysed by electrospray mass spectrometry (ES-MS and ES-MS/MS). For MS of phospholipids such as GPCho, SM, GPA, GPGro, cardiolipin, GPIno, GPEth and GPSer, samples were re-suspended in chloroform/

methanol (1:2 v/v). An aliquot of total lipid extract was analysed with a Micromass Quattro Ultima triple quadrupole mass spectrometer equipped with a nanoelectrospray source. Samples were loaded into thin-wall nanoflow capillary tips (Waters) and analysed by ES-MS in both positive and negative ion modes using a capillary voltage of 0.9 kV and cone voltages of 50 V. Tandem mass spectra (MS/MS) were obtained using argon as the collision gas (~3.0 mTorr) with collision offset energies as follows: 35 V, GPCho/SM in positive ion mode, parent ion scanning of m/z 184; 45 V, GPIno in negative ion mode, parent ion scanning of m/z 241; 45 V, GPEth in negative ion mode, parent ion scanning of m/z 196; 28 V, GPSer in negative ion mode, neutral loss scanning of m/z 87; and 40 V, for all glycerophospholipids (including GPA, GPGro and cardiolipin) detected by precursor scanning for *m/z* 153 in negative ion mode. MS/MS daughter ion scanning was performed with collision energies between 35 and 50 V. In positive ion mode, ions in the GPCho and SM spectra were annotated based on their [M + HNMe3(+)]+, [M-140] and [GPA-H] daughter ion derivatives, respectively, and compared with their theoretical values and previous analyses (Richmond and Smith, 2007). In negative ion mode, phospholipid class peaks were assigned according to their [lyso-H]–, [lyso-H20-H]–, [lysoGPA-H]– or [lysoGPA-H20-H]– daughter ion derivatives. Fatty acids were assigned based on their [M-H]– values. Saturated and unsaturated fatty acids were assumed to be esterified to the *sn*-1 and *sn*-2 position respectively. Annotation of all phospholipids is also based upon comparison to their theoretical values and other ES-MS and ES-MS/MS analyses conducted on whole-cell extracts (T.K. Smith, unpubl. data). Each spectrum encompasses at least 50 repetitive scans.

Total lipid inositol analysis

PCF trypanosomes (~1–5 × 10^8 cells), uninduced or induced for ACP RNAi (1, 2, 4, or 8 days), were harvested and washed in PBS. Lipids were extracted and analysed for inositol as previously described (Martin and Smith, 2006) with minor modifications. Briefly lipid extracts [chloroform: methanol (2:1 v/v) and chloroform:methanol:water (1:2:0.8 v/v)] were pooled, dried under nitrogen and stored at 4°C until they were subjected to base hydrolysis (concentrated NH_3 in 50% propan-1-ol, 50°C for 5 h) followed by repeated partitioning between butan-1-ol and water. An internal standard of D6 *myo*-inositol was added to both phases prior to hydrolysis by strong acid (6M HCl, 110°C), derivatization with trimethylsilyl esters and analysis by GC-MS, according to the method of Ferguson (1993). Soybean GPIno and IPC controls were processed in parallel.

Acknowledgements

We thank Dr Anton Horváth, Dr Petra Čermáková, Dr Zhenzhen Jia, Dr Paul Watkins, Dr Becky TuSekine, Dr Dan Raben, Dr Noreen Williams, Dr Silvia Brown, Dr Rob Jensen, Dr Soo Hee Lee, Dr Kimberly Paul, Gokben Yildirir and other members of our labs for discussion and other contributions to this project. We thank Dr Kathleen Gabrielson for the use of her O_2 electrode, Dr Wade Gibson for the use of his phosphorimager and Dr Charles Rock for providing pantothenamide compounds. This work was supported by NIH (Grant AI21334, PTE), the Grant Agency of the Czech Republic (204/06/1558) and the Czech Ministry of Education (LC07032 and 2B06129) (JL), and by a Wellcome Trust Senior Research Fellowship 067441 (TKS).

References

Beattie, D.S., Obungu, V.H., and Kiaira, J.K. (1994) Oxidation of NADH by a rotenone and antimycin-sensitive pathway in the mitochondrion of procyclic *Trypanosoma brucei brucei*. *Mol Biochem Parasitol* **64:** 87–94.

Birch-Machin, M.A., and Turnbull, D.M. (2001) Assaying mitochondrial respiratory complex activity in mitochondria isolated from human cells and tissues. *Methods Cell Biol* **65:** 97–117.

Birner, R., Burgermeister, M., Schneiter, R., and Daum, G. (2001) Roles of phosphatidylethanolamine and of its several biosynthetic pathways in *Saccharomyces cerevisiae*. *Mol Biol Cell* **12:** 997–1007.

Bleijerveld, O.B., Brouwers, J.F., Vaandrager, A.B., Helms, J.B., and Houweling, M. (2007) The CDP-ethanolamine Pathway and Phosphatidylserine Decarboxylation Generate Different Phosphatidylethanolamine Molecular Species. *J Biol Chem* **282:** 28362–28372.

Bligh, E.G., and Dyer, W.J. (1959) A rapid method of total lipid extraction and purification. *Can J Biochem Physiol* **37:** 911–917.

Bochud-Allemann, N., and Schneider, A. (2002) Mitochondrial substrate level phosphorylation is essential for growth of procyclic *Trypanosoma brucei*. *J Biol Chem* **277:** 32849–32854.

Bogdanov, M., and Dowhan, W. (1999) Lipid-assisted protein folding. *J Biol Chem* **274:** 36827–36830.

Bogdanov, M., Sun, J., Kaback, H.R., and Dowhan, W. (1996) A phospholipid acts as a chaperone in assembly of a membrane transport protein. *J Biol Chem* **271:** 11615–11618.

Braly, P., Simpson, L., and Kretzer, F. (1974) Isolation of kinetoplast-mitochondrial complexes from *Leishmania tarentolae*. *J Protozool* **21:** 782–790.

Bringaud, F., Riviere, L., and Coustou, V. (2006) Energy metabolism of trypanosomatids: adaptation to available carbon sources. *Mol Biochem Parasitol* **149:** 1–9.

Brody, S., Oh, C., Hoja, U., and Schweizer, E. (1997) Mitochondrial acyl carrier protein is involved in lipoic acid synthesis in *Saccharomyces cerevisiae*. *FEBS Lett* **408:** 217–220.

Brown, S.V., Hosking, P., Li, J., and Williams, N. (2006) ATP synthase is responsible for maintaining mitochondrial membrane potential in bloodstream form *Trypanosoma brucei*. *Eukaryot Cell* **5:** 45–53.

Brun, R., and Schonenberger (1979) Cultivation and in vitro cloning or procyclic culture forms of *Trypanosoma brucei* in a semi-defined medium. *Acta Trop* **36:** 289–292.

Čermáková, P., Verner, Z., Man, P., Lukeš, J., and Horváth, A. (2007) Characterization of the NADH: ubiquinone oxidoreductase (complex I) in the trypanosomatid *Phytomonas serpens* (Kinetoplastida). *FEBS J* **274:** 3150–3158.

Chang, T., Milne, K.G., Guther, M.L., Smith, T.K., and Ferguson, M.A. (2002) Cloning of *Trypanosoma brucei* and *Leishmania major* genes encoding the GlcNAc-phosphatidylinositol de-N-acetylase of glycosylphosphatidylinositol biosynthesis that is essential to the African sleeping sickness parasite. *J Biol Chem* **277:** 50176–50182.

Chaudhuri, M., Ajayi, W., and Hill, G.C. (1998) Biochemical and molecular properties of the *Trypanosoma brucei* alternative oxidase. *Mol Biochem Parasitol* **95:** 53–68.

Cronan, J.E., Fearnley, I.M., and Walker, J.E. (2005) Mammalian mitochondria contain a soluble acyl carrier protein. *FEBS Lett* **579:** 4892–4896.

Doering, T.L., Pessin, M.S., Hoff, E.F., Hart, G.W., Raben, D.M., and Englund, P.T. (1993) Trypanosome metabolism of myristate, the fatty acid required for the variant surface glycoprotein membrane anchor. *J Biol Chem* **268:** 9215–9222.

Edman, K., and Ericson, I. (1987) Phospholipid and fatty acid composition in mitochondria from spinach (*Spinacia oleracea*) leaves and petioles. A comparative study. *Biochem J* **243:** 575–578.

Effron, P.N., Torri, A.F., Engman, D.M., Donelson, J.E., and Englund, P.T. (1993) A mitochondrial heat shock protein from *Crithidia fasciculata*. *Mol Biochem Parasitol* **59:** 191–200.

Fahy, E., Subramaniam, S., Brown, H.A., Glass, C.K., Merrill, A.H., Jr, Murphy, R.C., *et al.* (2005) A comprehensive classification system for lipids. *J Lipid Res* **46:** 839–861.

Fang, J., and Beattie, D.S. (2002) Novel FMN-containing rotenone-insensitive NADH dehydrogenase from *Trypanosoma brucei* mitochondria: isolation and characterization. *Biochemistry* **41:** 3065–3072.

Fang, J., and Beattie, D.S. (2003a) Identification of a gene encoding a 54 kDa alternative NADH dehydrogenase in *Trypanosoma brucei*. *Mol Biochem Parasitol* **127:** 73–77.

Fang, J., and Beattie, D.S. (2003b) Alternative oxidase present in procyclic *Trypanosoma brucei* may act to lower the mitochondrial production of superoxide. *Arch Biochem Biophys* **414:** 294–302.

Ferguson, M.A.J. (1993) GPI membrane anchors: isolation and analysis. In *Glycobiology: A Practical Approach.* Fukuda, M., and Kobata, A. (eds). Oxford: IRL Press, pp. 349–383.

Figarella, K., Uzcategui, N.L., Beck, A., Schoenfeld, C., Kubata, B.K., Lang, F., and Duszenko, M. (2006) Prostaglandin-induced programmed cell death in *Trypanosoma brucei* involves oxidative stress. *Cell Death Differ* **13:** 1802–1814.

Gaigg, B., Simbeni, R., Hrastnik, C., Paltauf, F., and Daum, G. (1995) Characterization of a microsomal subfraction associated with mitochondria of the yeast, *Saccharomyces cerevisiae*. Involvement in synthesis and import of phospholipids into mitochondria. *Biochim Biophys Acta* **1234:** 214–220.

Gohil, V.M., Thompson, M.N., and Greenberg, M.L. (2005) Synthetic lethal interaction of the mitochondrial phosphatidylethanolamine and cardiolipin biosynthetic pathways in *Saccharomyces cerevisiae*. *J Biol Chem* **280:** 35410–35416.

González-Halphen, D., and Maslov, D.A. (2004) NADH-ubiquinone oxidoreductase activity in the kinetoplasts of the plant trypanosomatid *Phytomonas serpens*. *Parasitol Res* **92:** 341–346.

Gueguen, V., Macherel, D., Jaquinod, M., Douce, R., and Bourguignon, J. (2000) Fatty acid and lipoic acid biosynthesis in higher plant mitochondria. *J Biol Chem* **275:** 5016–5025.

Hill, G.C., and Cross, G.A. (1973) Cyanide-resistant respiration and a branched cytochrome system in Kinetoplastidae. *Biochim Biophys Acta* **305:** 590–596.

Hiltunen, J.K., Okubo, F., Kursu, V.A., Autio, K.J., and Kastaniotis, A.J. (2005) Mitochondrial fatty acid synthesis and maintenance of respiratory competent mitochondria in yeast. *Biochem Soc Trans* **33:** 1162–1165.

Horváth, A., Berry, E.A., and Maslov, D.A. (2000) Translation of the edited mRNA for cytochrome b in trypanosome mitochondria. *Science* **287:** 1639–1640.

Horváth, A., Horáková, E., Dunajčíková, P., Verner, Z., Pravdová, E., Šlapetová, I., *et al.* (2005) Downregulation of the nuclear-encoded subunits of the complexes III and IV disrupts their respective complexes but not complex I in procyclic *Trypanosoma brucei*. *Mol Microbiol* **58:** 116–130.

Jones, S.M., Urch, J.E., Kaiser, M., Brun, R., Harwood, J.L., Berry, C., and Gilbert, I.H. (2005) Analogues of thiolactomycin as potential antimalarial agents. *J Med Chem* **48:** 5932–5941.

Kastaniotis, A.J., Autio, K.J., Sormunen, R.T., and Hiltunen, J.K. (2004) Htd2p/Yhr067p is a yeast 3-hydroxyacyl-ACP dehydratase essential for mitochondrial function and morphology. *Mol Microbiol* **53:** 1407–1421.

Kuge, O., Nishijima, M., and Akamatsu, Y. (1991) A Chinese hamster cDNA encoding a protein essential for phosphatidylserine synthase I activity. *J Biol Chem* **266:** 24184–24189.

Lamour, N., Riviere, L., Coustou, V., Coombs, G.H., Barrett, M.P., and Bringaud, F. (2005) Proline metabolism in procyclic *Trypanosoma brucei* is down-regulated in the presence of glucose. *J Biol Chem* **280:** 11902–11910.

Law, R.H., Manon, S., Devenish, R.J., and Nagley, P. (1995) ATP synthase from *Saccharomyces cerevisiae*. *Methods Enzymol* **260:** 133–163.

Lee, S.H., Stephens, J.L., Paul, K.S., and Englund, P.T. (2006) Fatty Acid synthesis by elongases in trypanosomes. *Cell* **126:** 691–699.

Leray, C., Pelletier, X., Hemmendinger, S., and Cazenave, J.P. (1987) Thin-layer chromatography of human platelet phospholipids with fatty acid analysis. *J Chromatogr* **420:** 411–416.

Li, G., Chen, S., Thompson, M.N., and Greenberg, M.L. (2007) New insights into the regulation of cardiolipin biosynthesis in yeast: implications for Barth syndrome. *Biochim Biophys Acta* **1771:** 432–441.

Martin, K.L., and Smith, T.K. (2006) The glycosylphosphatidylinositol (GPI) biosynthetic pathway of bloodstream-form *Trypanosoma brucei* is dependent on the de novo synthesis of inositol. *Mol Microbiol* **61:** 89–105.

Maslov, D.A., Zíková, A., Kyselová, I., and Lukeš, J. (2002) A putative novel nuclear-encoded subunit of the cytochrome c oxidase complex in trypanosomatids. *Mol Biochem Parasitol* **125:** 113–125.

Masterson, W.J., Doering, T.L., Hart, G.W., and Englund, P.T. (1989) A novel pathway for glycan assembly: biosynthesis of the glycosyl-phosphatidylinositol anchor of the trypanosome variant surface glycoprotein. *Cell* **56:** 793–800.

McManus, M.T., Shimamura, M., Grams, J., and Hajduk, S.L. (2001) Identification of candidate mitochondrial RNA editing ligases from *Trypanosoma brucei*. *RNA* **7:** 167–175.

Menon, A.K., Eppinger, M., Mayor, S., and Schwarz, R.T. (1993) Phosphatidylethanolamine is the donor of the terminal phosphoethanolamine group in trypanosome glycosylphosphatidylinositols. *EMBO J* **12:** 1907–1914.

Mikhaleva, N.I., Golovastov, V.V., Zolov, S.N., Bogdanov, M.V., Dowhan, W., and Nesmeyanova, M.A. (2001) Depletion of phosphatidylethanolamine affects secretion of *Escherichia coli* alkaline phosphatase and its transcriptional expression. *FEBS Lett* **493:** 85–90.

Mikolajczyk, S., and Brody, S. (1990) De novo fatty acid synthesis mediated by acyl-carrier protein in *Neurospora crassa* mitochondria. *Eur J Biochem* **187:** 431–437.

Mileykovskaya, E.I., and Dowhan, W. (1993) Alterations in the electron transfer chain in mutant strains of *Escherichia coli* lacking phosphatidylethanolamine. *J Biol Chem* **268:** 24824–24831.

Morita, Y.S., Paul, K.S., and Englund, P.T. (2000) Specialized fatty acid synthesis in African trypanosomes: myristate for GPI anchors. *Science* **288:** 140–143.

Nagamune, K., Nozaki, T., Maeda, Y., Ohishi, K., Fukuma, T., Hara, T., *et al.* (2000) Critical roles of glycosylphosphatidylinositol for *Trypanosoma brucei*. *Proc Natl Acad Sci USA* **97:** 10336–10341.

Nerlich, A., von Orlow, M., Rontein, D., Hanson, A.D., and Dormann, P. (2007) Deficiency in phosphatidylserine decarboxylase activity in the psd1 psd2 psd3 triple mutant of *Arabidopsis* affects phosphatidylethanolamine accumulation in mitochondria. *Plant Physiol* **144:** 904–914.

Nigam, S., and Schewe, T. (2000) Phospholipase A(2)s and lipid peroxidation. *Biochim Biophys Acta* **1488:** 167–181.

Njogu, R.M., Whittaker, C.J., and Hill, G.C. (1980) Evidence for a branched electron transport chain in *Trypanosoma brucei*. *Mol Biochem Parasitol* **1:** 13–29.

Ondeyka, J.G., Zink, D.L., Young, K., Painter, R., Kodali, S., Galgoci, A., *et al.* (2006) Discovery of bacterial fatty acid synthase inhibitors from a *Phoma* species as antimicrobial agents using a new antisense-based strategy. *J Nat Prod* **69:** 377–380.

Opperdoes, F.R., and Borst, P. (1977) Localization of nine glycolytic enzymes in a microbody-like organelle in *Trypanosoma brucei*: the glycosome. *FEBS Lett* **80:** 360–364.

Patnaik, P.K., Field, M.C., Menon, A.K., Cross, G.A., Yee, M.C., and Butikofer, P. (1993) Molecular species analysis of phospholipids from *Trypanosoma brucei* bloodstream and procyclic forms. *Mol Biochem Parasitol* **58:** 97–105.

Paul, K.S., Bacchi, C.J., and Englund, P.T. (2004) Multiple triclosan targets in *Trypanosoma brucei*. *Eukaryot Cell* **3:** 855–861.

Richmond, G.S., and Smith, T.K. (2007) A novel phospholipase from *Trypanosoma brucei*. *Mol Microbiol* **63:** 1078–1095.

Rietveld, A.G., Koorengevel, M.C., and de Kruijff, B. (1995) Non-bilayer lipids are required for efficient protein transport across the plasma membrane of *Escherichia coli*. *EMBO J* **14:** 5506–5513.

Runswick, M.J., Fearnley, I.M., Skehel, J.M., and Walker, J.E. (1991) Presence of an acyl carrier protein in NADH: ubiquinone oxidoreductase from bovine heart mitochondria. *FEBS Lett* **286:** 121–124.

Sackmann, U., Zensen, R., Rohlen, D., Jahnke, U., and Weiss, H. (1991) The acyl-carrier protein in *Neurospora crassa* mitochondria is a subunit of NADH: ubiquinone reductase (complex I). *Eur J Biochem* **200:** 463–469.

Schagger, H., Hagen, T., Roth, B., Brandt, U., Link, T.A., and von Jagow, G. (1990) Phospholipid specificity of bovine heart bc1 complex. *Eur J Biochem* **190:** 123–130.

Schlame, M., Brody, S., and Hostetler, K.Y. (1993) Mitochondrial cardiolipin in diverse eukaryotes. Comparison of biosynthetic reactions and molecular acyl species. *Eur J Biochem* **212:** 727–735.

Schnaufer, A., Clark-Walker, G.D., Steinberg, A.G., and Stuart, K. (2005) The F1-ATP synthase complex in bloodstream stage trypanosomes has an unusual and essential function. *EMBO J* **24:** 4029–4040.

Schneider, R., Massow, M., Lisowsky, T., and Weiss, H. (1995) Different respiratory-defective phenotypes of *Neurospora crassa* and *Saccharomyces cerevisiae* after inactivation of the gene encoding the mitochondrial acyl carrier protein. *Curr Genet* **29:** 10–17.

Schneider, R., Brors, B., Massow, M., and Weiss, H. (1997) Mitochondrial fatty acid synthesis: a relic of endosymbiontic origin and a specialized means for respiration. *FEBS Lett* **407:** 249–252.

Shintani, D.K., and Ohlrogge, J.B. (1994) The characterization of a mitochondrial acyl carrier protein isoform isolated from *Arabidopsis thaliana*. *Plant Physiol* **104:** 1221–1229.

Smith, S. (1994) The animal fatty acid synthase: one gene, one polypeptide, seven enzymes. *FASEB J* **8:** 1248–1259.

Smith, T.K., Crossman, A., Brimacombe, J.S., and Ferguson, M.A. (2004) Chemical validation of GPI biosynthesis as a drug target against African sleeping sickness. *EMBO J* **23:** 4701–4708.

Speijer, D., Breek, C.K., Muijsers, A.O., Hartog, A.F., Berden, J.A., Albracht, S.P., *et al.* (1997) Characterization of the respiratory chain from cultured *Crithidia fasciculata*. *Mol Biochem Parasitol* **85:** 171–186.

Steenbergen, R., Nanowski, T.S., Beigneux, A., Kulinski, A., Young, S.G., and Vance, J.E. (2005) Disruption of the phosphatidylserine decarboxylase gene in mice causes embryonic lethality and mitochondrial defects. *J Biol Chem* **280:** 40032–40040.

Stephens, J.L., Lee, S.H., Paul, K.S., and Englund, P.T. (2007) Mitochondrial Fatty Acid Synthesis in *Trypanosoma brucei*. *J Biol Chem* **282:** 4427–4436.

Timms, M.W., van Deursen, F.J., Hendriks, E.F., and Matthews, K.R. (2002) Mitochondrial development during life cycle differentiation of African trypanosomes: evidence for a kinetoplast-dependent differentiation control point. *Mol Biol Cell* **13:** 3747–3759.

Torkko, J.M., Koivuranta, K.T., Miinalainen, I.J., Yagi, A.I., Schmitz, W., Kastaniotis, A.J., *et al.* (2001) *Candida tropicalis* Etr1p and *Saccharomyces cerevisiae* Ybr026p (Mrf1′, p.), 2-enoyl thioester reductases essential for mitochondrial respiratory competence. *Mol Cell Biol* **21:** 6243–6253.

Turrens, J.F. (1989) The role of succinate in the respiratory chain of *Trypanosoma brucei* procyclic trypomastigotes. *Biochem J* **259:** 363–368.
Voelker, D.R. (1997) Phosphatidylserine decarboxylase. *Biochim Biophys Acta* **1348:** 236–244.
Wakabayashi, T. (2002) Megamitochondria formation – physiology and pathology. *J Cell Mol Med* **6:** 497–538.
Wang, Z., and Englund, P.T. (2001) RNA interference of a trypanosome topoisomerase II causes progressive loss of mitochondrial DNA. *EMBO J* **20:** 4674–4683.
Wang, Z., Morris, J.C., Drew, M.E., and Englund, P.T. (2000) Inhibition of *Trypanosoma brucei* gene expression by RNA interference using an integratable vector with opposing T7 promoters. *J Biol Chem* **275:** 40174–40179.
Wang, J., Soisson, S.M., Young, K., Shoop, W., Kodali, S., Galgoci, A., *et al.* (2006) Platensimycin is a selective FabF inhibitor with potent antibiotic properties. *Nature* **441:** 358–361.
van Weelden, S.W., Fast, B., Vogt, A., van der Meer, P., Saas, J., van Hellemond, J.J., *et al.* (2003) Procyclic *Trypanosoma brucei* do not use Krebs cycle activity for energy generation. *J Biol Chem* **278:** 12854–12863.
van Weelden, S.W., van Hellemond, J.J., Opperdoes, F.R., and Tielens, A.G. (2005) New functions for parts of the Krebs cycle in procyclic *Trypanosoma brucei*, a cycle not operating as a cycle. *J Biol Chem* **280:** 12451–12460.
Zhang, W., Campbell, H.A., King, S.C., and Dowhan, W. (2005) Phospholipids as determinants of membrane protein topology. Phosphatidylethanolamine is required for the proper topological organization of the gamma-aminobutyric acid permease (GabP) of *Escherichia coli*. *J Biol Chem* **280:** 26032–26038.
Zhang, Y.M., Frank, M.W., Virga, K.G., Lee, R.E., Rock, C.O., and Jackowski, S. (2004) Acyl carrier protein is a cellular target for the antibacterial action of the pantothenamide class of pantothenate antimetabolites. *J Biol Chem* **279:** 50969–50975.
Zíková, A., Horáková, E., Jirků, M., Dunajčíková, P., and Lukeš, J. (2006) The effect of down-regulation of mitochondrial RNA-binding proteins MRP1 and MRP2 on respiratory complexes in procyclic *Trypanosoma brucei*. *Mol Biochem Parasitol* **149:** 65–73.

Supplementary material

This material is available as part of the online article from:
http://www.blackwell-synergy.com/doi/abs/10.1111/j.1365-2958.2008.06112.x
(This link will take you to the article abstract).

Please note: Blackwell Publishing is not responsible for the content or functionality of any supplementary materials supplied by the authors. Any queries (other than missing material) should be directed to the corresponding author for the article.

